Development of large size fast timing and radiation resistant PVT-based plastic scintillator detector

Lizbeth Alex[1], Rajesh Paulraj[1,*] , Sonu[2], and Mohit Tyagi[2]

[1] Centre for Crystal Growth, Department of Physics, Sri Sivasubramaniya Nadar College of Engineering, Kalavakkam, Chennai, Tamil Nadu 603110, India
[2] Crystal Technology Section, Technical Physics Division, Bhabha Atomic Research Centre, Mumbai 400085, India

ABSTRACT

The fabrication and the scintillation properties of a polyvinyltoluene-based plastic scintillator doped with 2,5-diphenyloxazole (PPO) and 1,4-bis[2-(phenyloxazolyl)]-benzene (POPOP) are presented. The XRD structural analysis and SEM-EDS technique confirm the amorphous nature of the material. The high optical transparency of 88% over the entire visible region, the refractive index of 1.57 near to that of glass and the emission wavelength at 425 nm make the synthesized PVT scintillator well suitable for radiation detection and measurements. The scintillation lifetime of 4 ns under ^{137}Cs exposure revealed its utilization as fast timing detector for Time-of-Flight measurements. The fabricated scintillator shows a maximum light output of 65% of stilbene crystal. Scintillation light loss shown for ^{60}Co irradiations with radiation doses of 1 Mrad and 1.98 Mrad evinced the good radiation hardness characteristic of the material, bringing about a best candidate for high radiation level environments.

1 Introduction

Scintillation detectors are the oldest techniques known for the accurate detection and spectroscopy of a broad range of radiations. The scintillation light produced by the materials, when excited by ionizing radiation, is then coupled with a photodetector (such as photodiodes, PMTs etc.) which converts them into electrical signals. These signals can be further analyzed and counted to quantify and identify the incident radiation. Organic scintillators took a noticeable position in the field of scintillation detection as a fast radiation detector, due to their fast response time and fairly high light output. Plastic scintillators are now a days the most widely accepted organic detectors besides liquid and crystalline ones, due to its rapid decay time, moderately high relative light yield, environmental stability, low toxicity, ease of handling and production of large volumes at cheap rates [1–4].

Despite low density and efficiency compared to inorganic counterparts, the prompt scintillation decay time and the cost-effective large volume size of the plastic scintillator have led to their extensive utilization in security applications, dosimetry, and high-energy physics [5]. They are diagnosed as fast neutron detectors because of their high hydrogen

content. These new solid-state materials are also a good alternative to liquid scintillators, which have been used for decades as fast neutron detectors, mainly due to its drawbacks such as difficulty in handling, toxicity, disposal, and presence of dissolved oxygen that can reduce the fluorescence intensity and further limits the performance efficiency [6, 7].

High purity of the starting materials, selection of monomers and fluors, its solubility, the synthesis method (Thermal Polymerization), optical properties, etc. strongly affect the light output of the plastic scintillator. Wavelength shifters are used to match the emission wavelength of the plastic scintillator with that of the quantum efficiency of the photomultiplier tubes (PMTs) used and hence to increase the attenuation length. Thermal polymerization condition (100–150 °C for a certain period of days) results in polymers with higher molecular weights [8] which displays higher light yield compared to scintillators consisting of polymers with shorter chains [9]. Optical parameters, which include self-absorption, extraction of photons, surface polishing, optical coupling between the scintillator and the PMT, etc. show a great impact on the final response of the scintillator [6, 10]. The analysis of Zhu et al. [11] revealed that the 2 wt% of fluorescent dye PPO doped in polystyrene shows higher fluorescence intensity, improved scintillation efficiency and good light yield and increasing the concentration above this optimum value decreased the light output by quenching effect. The report by Molisch et al. [12] evaluated that the increase in the dopant concentration also increased the lifetime of the scintillation light due to radiation trapping. The concentration of the wavelength shifting luminescent additives can have a great influence on maximizing the scintillation efficiency. The studies conducted by Adadurov et al. [13] found out that the optimal concentration of the POPOP spectral shifter should be decreased for large dimensional plastic scintillators to avoid self-absorption which leads to light losses in the material. Plastic scintillators are vulnerable to radiation damage, which in due course decreases the light output by the generation of absorption centers and the degradation of fluors [14]. Their radiation resistance mainly relies on factors such as temperature, presence of oxygen, total absorbed dose, and dose rate.

The present study has been focused on the development of large size fast timing and radiation resistant polyvinyltoluene (PVT)-based plastic scintillator detector doped with optimized concentrations of 2 wt% 2,5-diphenyloxazole (PPO) and 0.05 wt% 1,4-bis[2-(phenyloxazolyl)]-benzene (POPOP). The structural analysis and the surface morphology were investigated using XRD and SEM-EDS techniques. The luminescence spectrum shows the emission wavelength lying in the visible region. Gamma-ray spectroscopy was performed with ^{137}Cs, ^{60}Co, and ^{22}Na gamma-ray sources and the energy calibration was done. The decay time of the fabricated scintillator was determined and the relative light yield was estimated in comparison to organic stilbene crystal under the similar experimental parameters. Radiation hardness was measured under normal conditions (air, room temperature) and the scintillation efficiency loss in relation to the absorbed dose and the recovery of the irradiated scintillator were examined.

2 Experimental details

2.1 Synthesis of plastic scintillator

Polyvinyltoluene-based plastic scintillator was synthesized using thermal polymerization. The vinyltoluene monomer, the primary dopant 2,5-diphenyloxazole (PPO), and the wavelength shifter 1,4-bis[2-(phenyloxazolyl)]-benzene (POPOP) were purchased from Sigma-Aldrich with 99.5% purity. The monomer was further purified to remove the inhibitors and particulates present. This was done by adding a prepared mixture of 3 g sodium hydroxide (NaOH) with 100 cc distilled water to vinyltoluene and kept aside for about 15 min for complete separation. This process was repeated several times to attain thorough purification.

The distilled vinyltoluene was mixed with the dopants and the nitrogen gas was used to degas the solution through bubbling method. The homogeneously stirred solution was then transferred into a cylindrical vial (20 mm diameter and 80 mm height) and closed inside the glove box. The sealed vial was placed in a high-temperature heater for about a period of 10 days to perform polymerization reaction at a temperature of 120 °C. Figure 1a and b shows the synthesized plastic scintillator samples under white and UV light.

The fabricated scintillator was cut by South Bay Tech-low speed Diamond wheel cutter and polishing was done using 320–1500 grit sandpapers and with diamond paste of 0.5 micron using a suitable velvet cloth. The perfectly polished sample was finally covered with Teflon Tape for further protection.

2.2 Scintillation measurements

Radioluminescence was measured using an X-ray source for excitation at room temperature with voltage and current kept at 150 kV and 4 mA respectively. A spectrograph (Avaspec 3648) coupled to an optical fiber was used to record the emission spectrum over an integration time of 5 s.

Pulse height spectra and energy calibration were acquired by irradiating the plastic scintillator with gamma-rays from ^{137}Cs, ^{60}Co, and [22]Na sources. The polished surface of the sample was coupled with Hamamatsu R877-100 PMT using optical grease for better optical coupling and covered with spectralon to reflect the emitted photons towards the PMT window. The detector was fully closed with aluminium foil and the PMT's signal output was connected to a preamplifier and then to a spectroscopic amplifier. The spectra were analyzed using the Tukan 8k multichannel analyzer with a shaping time optimized to be of 0.5 μs to reduce the incidence of pulse 'pile up', to improve the signal-to-noise ratio and for better resolution.

Scintillation decay time was determined by coupling the scintillator with Hamamatsu H3378-50 PMT, where the output was directly fed to a digital Tektronix oscilloscope MDO3102. The relative light yield was estimated by comparing the position of the Compton edge in the pulse height spectra from the ^{137}Cs source of the plastic scintillator to that of the stilbene crystal.

Radiation hardness studies were performed by irradiating the sample with ^{60}Co in a Blood Irradiator-2000 at a dose rate of 700 rad/min. The samples were first exposed to a radiation dose of 1 Mrad and then exposed to an additional dose of 0.98 Mrad, for a cumulative exposed radiation dose of 1.98 Mrad. Measurements were taken on the sample immediately after the irradiation.

3 Results and discussions

3.1 X-ray diffraction (XRD)

The XRD pattern of the synthesized PVT- based plastic scintillator was analyzed using the Proto AXRD_LPD_HR X-Ray diffraction system. The data was recorded in the ranges between $2\theta = 2°–80°$ with a step size of 0.2°. The Cu X-ray tube was used as the X-ray source, having an accelerating voltage of 40 kV and a tube current of 3mA. Figure 2 shows two broad halo humped diffraction peaks extending between $2\theta = 5°–14°$ and $2\theta = 35°–55°$, proving the amorphous nature of the plastic scintillator. These two broader amorphous signals may be due to two different chain's length and the orientation, indicating the presence of two different amorphous phases of the material [15, 16].

3.2 Scanning electron microscopy (SEM)

SEM is a convenient characterization technique to know the surface morphology and also the

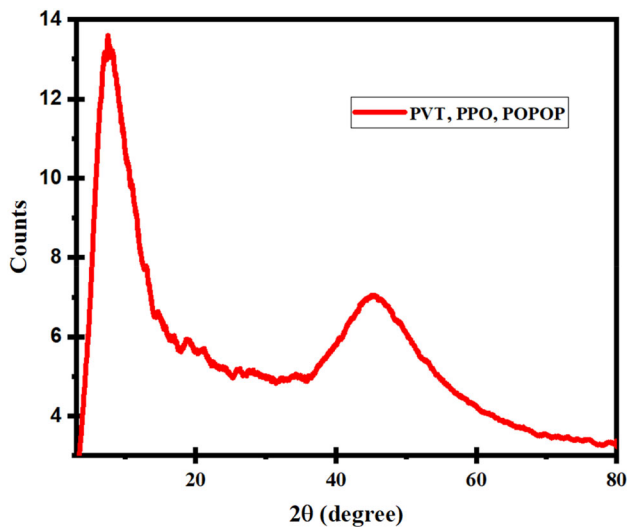**Fig. 1** **a** and **b** Photographs of fabricated scintillators under white and UV illumination
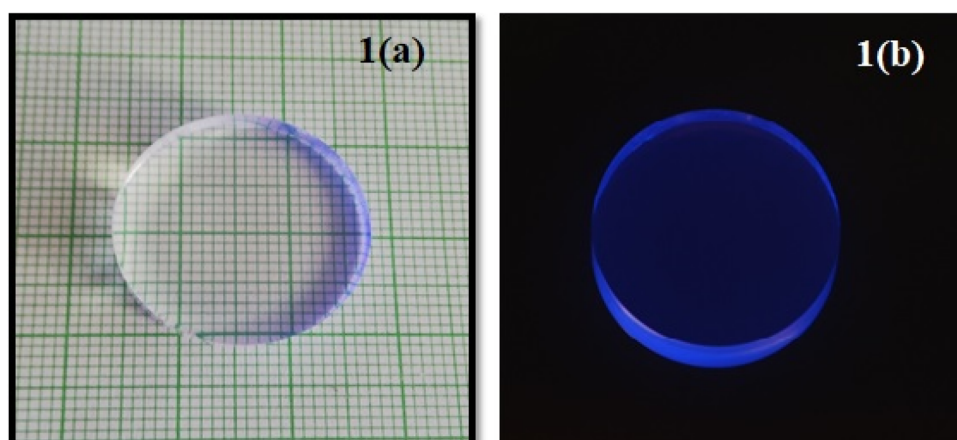
Fig. 2 X-ray diffraction pattern of the PVT-based plastic scintillator

distribution of particles in polymer composites, nanocomposites [17, 18] as well as in hybrid materials [19]. The microstructural morphology of 2 wt% PPO and 0.05 wt% POPOP loaded polyvinyltoulene based plastic scintillator sample was analyzed using Thermosceintific Apreo S HRSEM and the elemental compositions were measured using energy dispersive X-ray spectroscopy (EDX) on SNE3200M tabletop scanning electron microscope after chromium sputtering. An operating voltage of 5 kV was selected for SEM recording based on the information required and the low atomic number nature of the synthesized plastic scintillator [20].

The high-resolution scanning electron microscope (HRSEM) image of the PPO and POPOP loaded PVT-based plastic scintillator is shown in Fig. 3a. The uniformly dispersed small grain like microstructural arrangement can be observed for the plastic scintillator sample, rendering it to be amorphous. This is also predicted from the broader halo peak obtained by the XRD analysis [19, 20]. The EDS spectroscopy confirmed the presence of C and O in the material (Fig. 3b). The negligible percentage of Al observed is due to the impurities present in the specimen holder. Table 1. shows the elemental compositions in weight% for the PPO and POPOP loaded plastic scintillator obtained from the energy dispersive X-ray spectroscopy (EDX) measurements.

3.3 Optical transmittance

The optical transmittance plays a significant role in the measurement of light yield of the scintillator, as it depends on how much amount of the scintillation light from the spectral shifter that enters the photodetector. Good transmittance allows the better propagation of the scintillation light through the material and also reduces the phenomenon of self-absorption [21]. The UV–Vis NIR transmittance spectrum of the PVT-based plastic scintillator doped with PPO and POPOP (2 mm thickness) recorded using UV–Vis NIR spectrophotometer within the wavelength range from 300 to 1000 nm is shown in Fig. 4. The graph displays that the material exhibits high transmittance (i.e., good optical quality) all over the visible region with a transparency of 88%, making it applicable for scintillation measurements [22]. The lower cut-off wavelength of the synthesized scintillator is shown to be at 400 nm.

3.4 Refractive index

Brewster's angle method (model HO-ED-P-01) was used to examine the index of refraction of the synthesized PVT-based plastic scintillator. The apparatus in the experiment comprises of a diode laser of wavelength 650 nm (input power = 230 V and output power = 3mW), polarizer with an accuracy of 2°/division, optical rail (length = 500 mm), goniometer of resolution 1″ and pinhole photodetector (diameter = 0.7 mm) connected to a detector output digital measurement unit. The experimental setup and the procedure were explained in detail by Kamalesh et al. [23]. The optically transparent plastic scintillator sample of thickness 2 mm was used for the study. The angle of rotation versus the detector output (i.e., intensity of the reflected beam from the sample) was plotted, as shown in the Fig. 5. The refractive index was determined using the following Eqs. [24],

$$\mu = \tan i_p \qquad (1)$$

where μ is the refractive index and i_p is the Brewster's angle or polarizing angle (θ_p).

The Brewster's angle i_p is found to be 57.5°, where the output intensity is minimum and the refractive index μ is 1.57 for the PVT-based plastic scintillator.

Fig. 3 **a** SEM image of the PVT-based plastic scintillator and **b** EDS of PPO and POPOP loaded plastic scintillator
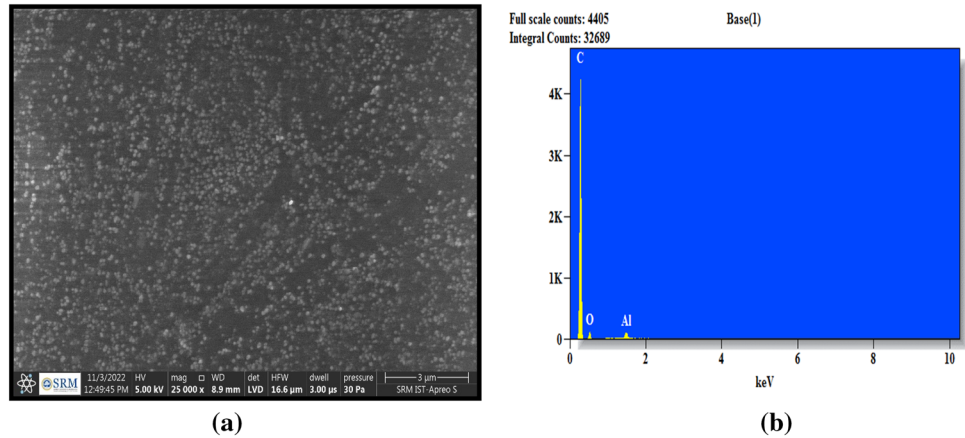

(a)   (b)

Table 1 Weight% of elements in the PPO and POPOP doped PVT scintillator

Sl. no.	Element	Net counts	Weight%	Atom %
1	C	23,766	79.47	84.23
2	O	797	18.78	14.94
3	Al	886	1.76	0.83
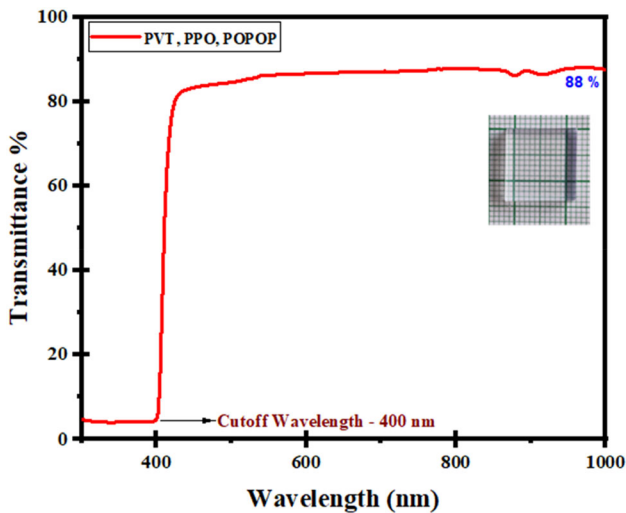
Fig. 4 UV–Vis NIR transmittance spectrum of the PVT-based plastic scintillator doped with 2% PPO and 0.05% POPOP.

The index of refraction is near to that of glass (~ 1.5), which allows the efficient coupling of the scintillation light of the plastic scintillator to that of the photomultiplier tube used [22].
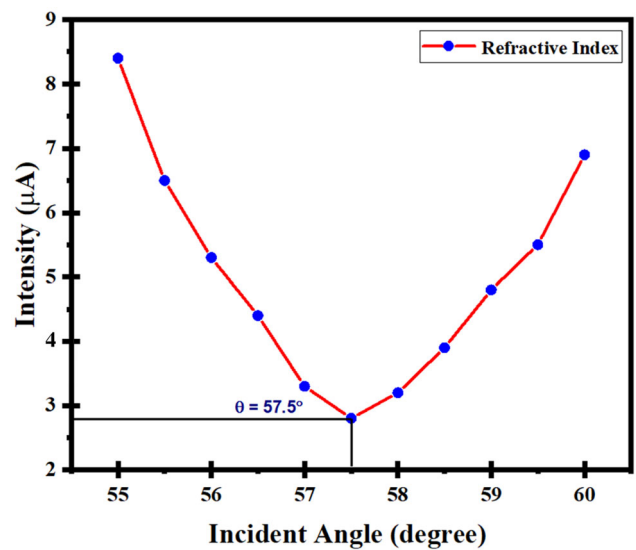

Fig. 5 Plot of angle of rotation versus the detector output

3.5 Radioluminescence

The radioluminescence spectra of polyvinyltoluene doped with 2 wt% 2,5-diphenyloxazole (PPO) and 0.05 wt% 1,4-bis[2-(phenyloxazolyl)]-benzene (POPOP) is shown on Fig. 6. The spectrum was acquired by analysing the radiation emitted by the face opposite to that which was directly excited. It is known that fluorescence intensity increases with higher transparency of the plastic scintillators [25]. As the overlapping between the optical absorption and emission spectra (referred to as Stokes shift) is very little, the probability of re-absorption of the emitted light in the scintillation material is smaller. Since the Stokes shift of POPOP is large (about
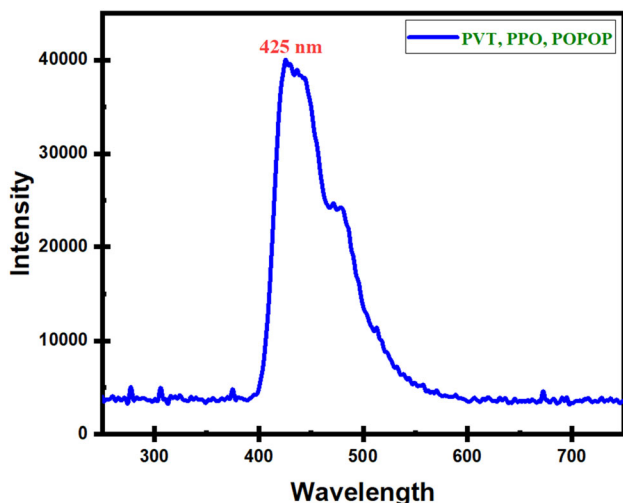
Fig. 6 Radioluminescence spectra of PVT doped with 2% PPO and 0.05% POPOP

50 nm), it is used as a wavelength shifter to increase the attenuation length [26].

The spectrum comprises a broad emission band between the regions of 400 and 600 nm under X-ray excitation, with a peak maximum at 425 nm, agreeing well with the scintillation emission of a typical plastic scintillator [27]. This is due to the π–π^{*} transition of the π-electrons in the carbon double bond. Here the emission accounts for the radiation transfer of energy from the excited polymer base (vinyltoluene) to the molecules of the primary fluor PPO and then from those to that of the secondary dopant or the wavelength shifter POPOP [28].

3.6 Pulse height Spectra

Figure 7 shows the schematic of the experimental setup for the pulse height spectra measurements of the synthesized plastic scintillator. The pulse height spectra for Cesium-137, Cobalt-60, and Sodium-22 measured with the synthesized plastic scintillator doped with 2,5-diphenyloxazole (PPO) and 1,4-bis[2-(phenyloxazolyl)]-benzene (POPOP) is depicted in Fig. 8. The gamma interactions that occur mainly in plastic scintillators are Compton scattering which can deposit only a fraction of its incident gamma-ray energy as a result of its low atomic number (i.e., low photoelectric interaction probability), so full-energy peaks cannot be seen in their pulse height spectra [22]. The kind of detector, the energy, and the nature of gamma-ray sources have a strong influence on the

behavior of these spectra [29, 30]. The type and the concentration of the fluorescent dyes (i.e., primary fluors and spectral shifters) incorporated also play a prominent role for the higher radiation detection efficiency (such as gamma and neutron detection) in the scintillation detectors. The scintillation light yield increases with the increase of incident energy, as the interaction of the photons are encouraged and thus, the spectrum gets extended to the higher channel number [31]. It is found that a larger number of output photons is obtained for the sample radiated by Cobalt-60 than compared to Cesium-137 and Sodium-22.

3.6.1 Energy calibration

Gamma sources such as ^{137}Cs, ^{60}Co, ^{22}Na are generally used for the energy calibration of the scintillator material by measuring the Compton edge, which corresponds to the maximum energy transferred during the backscattering of the gamma rays to the electron [32]. The Compton edge energy for each gamma source was calculated, based on their gamma-ray energies [33]. Since the ^{60}Co source emits two gamma rays of energies 1.17 MeV and 1.33 MeV, the Compton edge energy calculations were done by selecting the average energy. Table 2 gives the calculated Compton edge energy values of the corresponding gamma-ray sources.

Table 2 calculated compton edge values of the corresponding gamma sources.

One of the perfectly polished surfaces of the fabricated plastic scintillator was attached to the PMT window (Hamamatsu R877-100, Operating voltage, 1300 V) using optical grease and the other surface was covered with Teflon tape for reflecting the emitted photons towards the surface coupled to PMT. The spectra were recorded by using Tukan 8K multichannel analyzer over a measurement time of 900 s. The channel corresponding to the Compton edge energy of the spectra was identified by selecting the middle point where the slope falls down to one-half of the value of the Compton peak. The energy calibration result of the fabricated scintillator is as follows:

Fig. 7 The experimental setup for measuring the Compton edge spectra of the fabricated scintillator
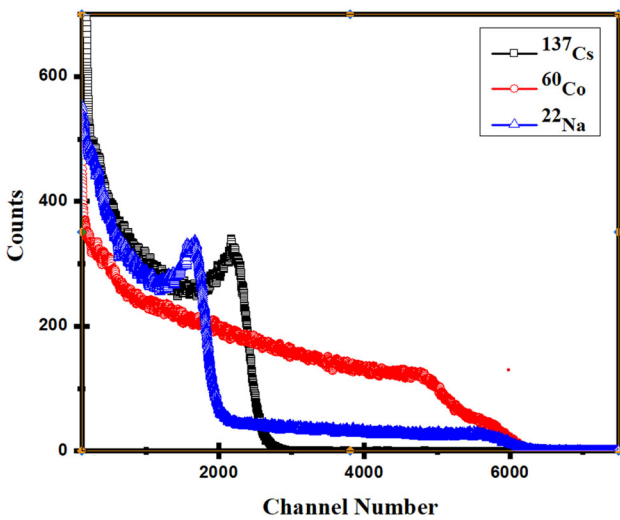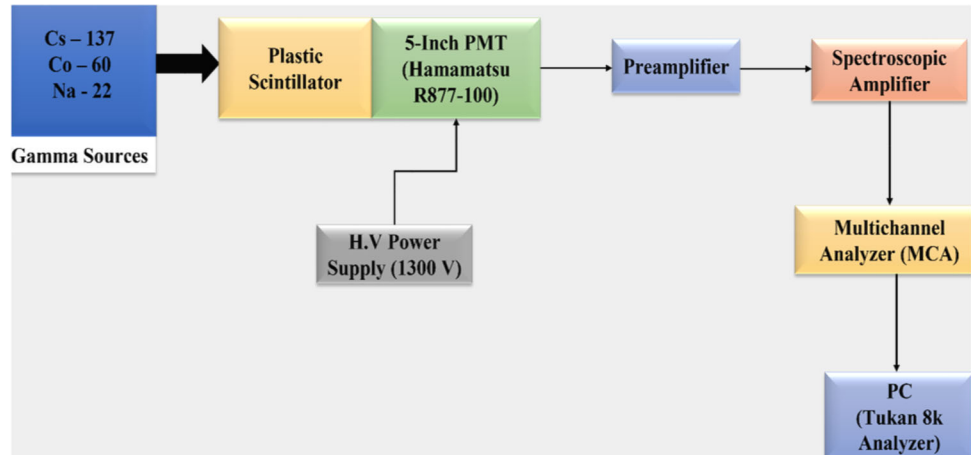

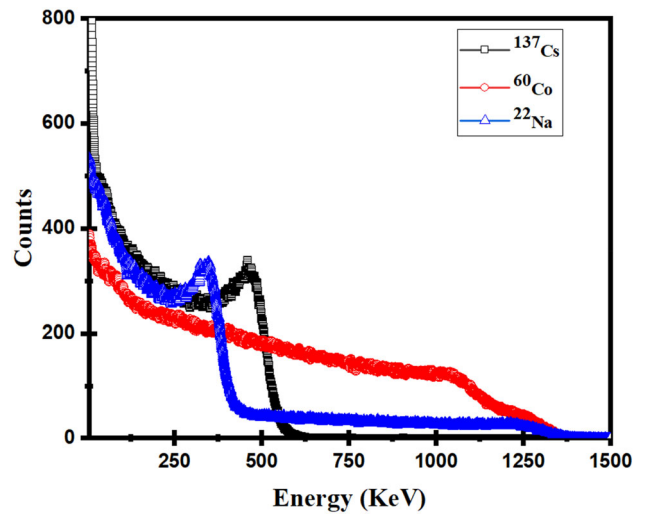**Fig. 8** Pulse height spectrum of the sample for three different gamma sources

Fig. 9 Gamma-ray pulse spectra after energy calibration

Table 2 Compton edge energy values of the three gamma-ray sources

SL.No.	Source	Gamma energy (keV)	Compton edge energy (keV)
1	Sodium 22 (^{22}Na)	511	340.1
2	Cobalt 60 (^{60}Co)	1173/1332	Avg. 1040.7
3	Cesium 137 (^{137}Cs)	661.6	477.3

$$\text{Channel No.} = 115.1343 + 4.48207 \times \text{energy} \ (R^2 = 99.919) \tag{2}$$

The gamma ray spectra of ^{137}Cs, ^{60}Co, ^{22}Na after energy calibration is shown in Fig. 9.

The fabricated plastic scintillator possesses excellent energy linearity of 99.9% through the energy calibration (Fig. 10). Thus, the results confirm that the response of the scintillator is proportional to the incident energy in the low gamma-ray energy region [32].

3.7 Scintillation decay

The decay characteristics of pulses under gamma-ray excitation in polyvinyltoluene based plastic scintillator doped with 2 wt.% 2,5-diphenyloxazole (PPO) and 0.05 wt.% 1,4-bis[2-(phenyloxazolyl)]-benzene (POPOP) is presented in Fig. 11. The lifetime of the
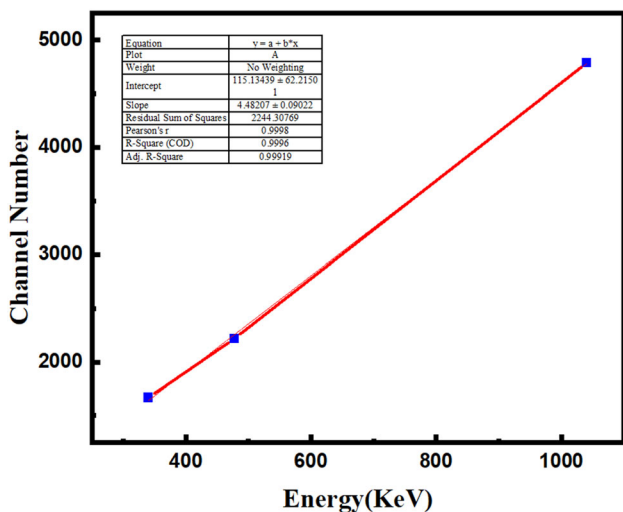
Fig. 10 Linear fit for the data points corresponding to the Compton edges for three gamma-ray sources of the fabricated scintillator
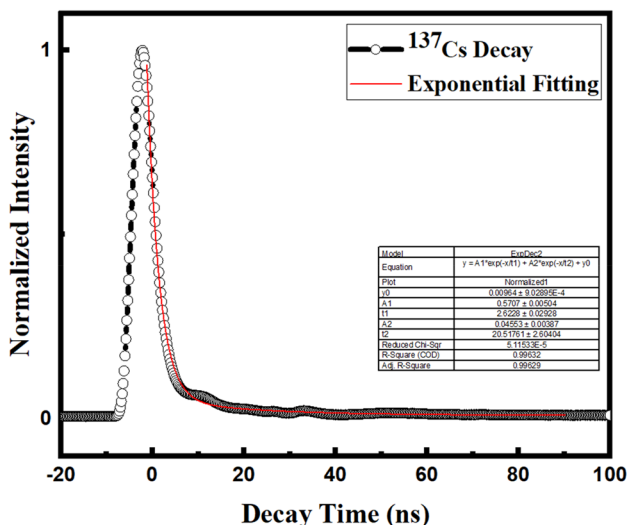

Fig. 11 Scintillation decay of polyvinyltoluene-based plastic scintillator under ^{137}Cs gamma-ray excitation

scintillation decay increases for higher PPO concentrations due to self-absorption [34]. The anode signals from the PMT (Hamamatsu H3378-50) coupled to the scintillator were recorded using a digital Tektronix oscilloscope MDO3102 having 1 GHz bandwidth.

The decay time spectra were fitted with a two-component exponential decay using the following equation:

$$I(t) = A_0 + A_1 \exp(-t/\tau_1) + A_2 \exp(-t/\tau_2) \quad (3)$$

where A_1, A_2 are the amplitudes and τ_1, τ_2 denote the time constants.

The ratio of relative amplitudes of the decay components was calculated with the equation:

$$Q_1 = \frac{A_1\tau_1}{A_1\tau_1 + A_2\tau_2} \quad (4)$$

The average decay time was evaluated to be 4 ns from the equation:

$$\tau_{\mathrm{avg}} = \frac{A_1\tau_1 + A_2\tau_2}{A_1 + A_2} \quad (5)$$

The fabricated plastic scintillator shows a fast response time compared to commercially available ones such as BC-428, BC-430, BC-416 [35].

3.8 Relative light yield

Light yield, an important characteristic of scintillators, corresponds to the number of photoelectrons per energy unit. Concentration quenching can decrease the scintillation light efficiency when the fluor concentration is increased above an optimum value, by reason of the generation of non-radiative energy transfer [31].

The Compton edge in the gamma-ray spectrum is found to be an alternate method for characterizing the relative light yield of the developed plastic scintillator [36]. This is achieved by comparing the Compton edge position in the pulse height spectrum for the 662 keV gamma-ray energy of ^{137}Cs of the synthesized plastic scintillator to that of the well-known organic crystal stilbene, measured under identical conditions such as measurement geometry, photomultipliers, and recording instruments (shown in Fig. 12). The shaping time applied for acquiring these spectra was 0.5 μs.

The fabricated plastic scintillator exhibits a light yield of 65% of the light output of stilbene (10,500 ph/MeV) [37].

3.9 Radiation hardness

The radiation resistance of the plastic scintillator depends not only on the polymer matrix but also on the fluorescent dyes and its concentration. The radiation damage process in scintillators is influenced by many parameters such as the nature of the irradiating particle (its stopping power), the amount of radiation dose absorbed, the rate of irradiation and the environmental conditions under which the radiation
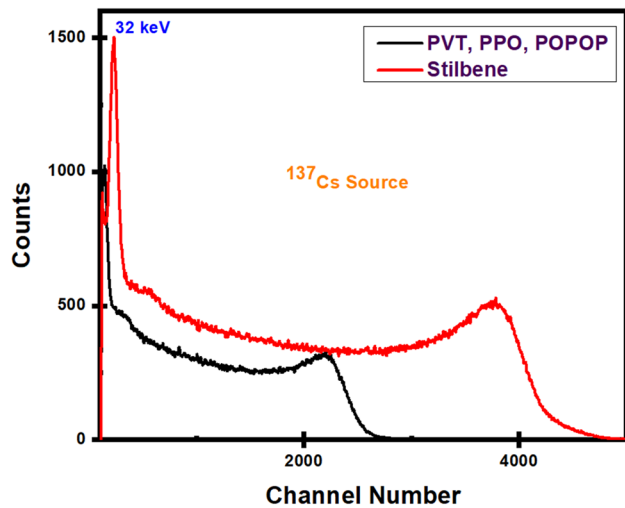
Fig. 12 Gamma-ray spectrum of the plastic scintillator from ^{137}Cs source relative to stilbene organic crystal

Fig. 13 Pulse height data of the PVT-based scintillator before irradiation and after 1 Mrad and 1.98 Mrad radiation doses

takes place [38, 39]. One of the main effects of this damage is that it can change the optical properties of the scintillator material. This is by decreasing the scintillation light output due to the damage caused to the fluorescent compounds or either through degrading the transmission behavior as a result of the formation of optical absorption centers. This eventually affects the light attenuation length of the scintillator [40]. Scintillation light yield loss due to the formation of color centres (or radiation traps) is less evident in long-wavelength regions than in UV and blue wavelength regions, after irradiation. So, wavelength shifters with large stokes shift are mostly used to improve the radiation hardness of the material [14].

The radiation damage studies of PVT-based plastic scintillator doped with 2 wt% 2,5-diphenyloxazole (PPO) and 0.05 wt% 1,4-bis[2-(phenyloxazolyl)]-benzene (POPOP) was analysed using the ^{60}Co source with a total radiation dose of 1.98 Mrad at a dose rate of 700 rad/min. The gamma-induced pulse height spectra of pre-irradiated and irradiated PVT-based scintillator (immediately after irradiation) are shown in Fig. 13. The values were determined by identifying the channel number corresponding to the Compton edge position of the gamma-ray spectrum. The relative scintillation efficiency is obtained by dividing the channel number by that value of the non-irradiated sample.

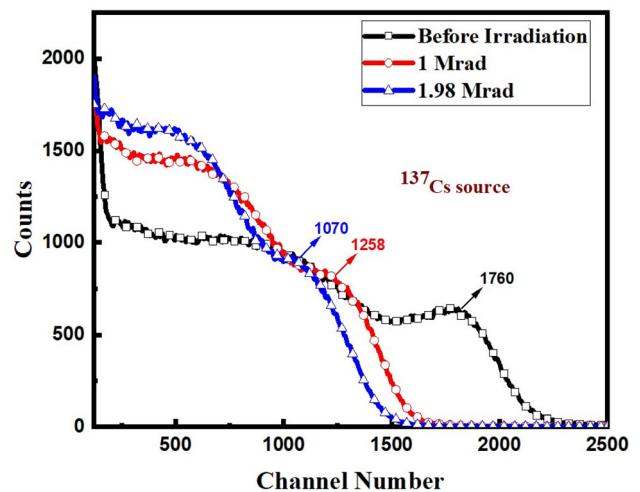At 1 Mrad radiation dose, the sample suffers 28% light loss and after 1.98 Mrad, the total scintillation

light loss is 39%. This is determined by comparing the Compton edge positions of the pulse height spectrum before and after irradiations.

Figure 14 presents the pulse height spectra during the recovery period by storing the sample in air atmosphere (i.e., by exposure to oxygen) at room temperature. The free radicals present react with the oxygen to give out peroxide radicals, which basically do not absorb the visible light and thus leads to bleaching [39]. The damage can be recovered in course of time, as it is not totally permanent. The recovery curve shown in Fig. 14 shows excellent recovery within 2 days of exposure to dry air atmosphere (an increase of 25% light yield), which makes
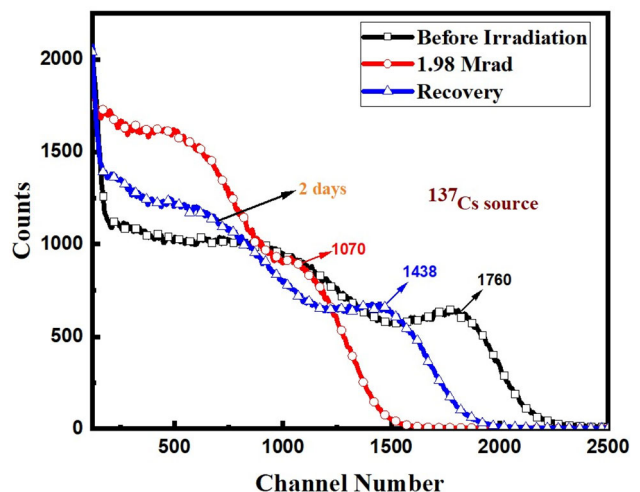

Fig. 14 Pulse height spectra of the irradiated sample after exposure to air atmosphere (recovery period)

it suitable for use in high-radiation environments [41]. Thus, the PVT-based plastic scintillator doped with PPO and POPOP has good radiation hardness characteristics, when compared to a standard plastic scintillator BC-408, which suffers 40% light yield loss at 1 Mrad radiation dose [42].

4 Conclusion

We have synthesized a large size optical transparent 2,5-diphenyloxazole (PPO) and 1,4-bis[2-(phenyloxazolyl)]-benzene (POPOP) doped polyvinyltoluene-based plastic scintillator using thermal polymerization reaction. The broad halo hump peak obtained in the XRD analysis predicts the amorphous nature of the material. The surface morphology and the elemental compositions were examined from the SEM-EDS technique. The X-ray excited luminescence spectrum shows an emission peak at 425 nm, which lies in the visible region of the electromagnetic spectrum. The fabricated scintillator exhibits an energy linearity of 99.9%. The short decay time of 4 ns under gamma-ray excitation of the scintillator marks its significance in fast timing measurements and in particle physics. The results of gamma-ray spectroscopy under gamma-ray sources such as ^{137}Cs, ^{60}Co, and ^{22}Na show that the synthesized scintillator possesses higher light output and the relative light yield is estimated to be 65% of that of stilbene crystal. The fabricated scintillator owns higher radiation resistance than the commercially available plastic scintillator BC-408. Thus, it can be concluded that the fabricated PVT- based plastic scintillator is an invaluable organic scintillation detector that can be used for radiation detection, homeland security, high radiation level environments and in high energy physics applications.

Author contributions

LA: material preparation, data collection and analysis, writing—original draft. RP: conceptualization, funding acquisition, supervision, project administration. S: visualization, data analysis. MT: visualization, investigation, writing—review and editing. The authors certify that this article has not been submitted or published in any other publications. The order of authors listed in the manuscript has been approved by all of them.

Data availability

The authors confirm that all the relevant data supporting the findings of the study are included in the submitted manuscript and any further data clarifications are available from the corresponding author, upon reasonable request.

Declarations

Conflict of interest   There are no conflicts to declare.

References

1. J.B. Birks, *The Theory and Practice of Scintillation Counting: International Series of Monographs in Electronics and Instrumentation*, vol. 27 (Elsevier, Amsterdam, 2013)
2. E.R. Siciliano, J.H. Ely, R.T. Kouzes, B.D. Milbrath, J.E. Schweppe, D.C. Stromswold, Comparison of PVT and NaI (tl) scintillators for vehicle portal monitor applications. Nucl. Instrum. Methods Phys. Res. A **550**(3), 647–674 (2005)
3. E. Montbarbon, Z. Zhang, A. Grabowski, R. Woo, D. Tromson, C. Dehé-Pittance, R.B. Pansu, G.H. Bertrand, M. Hamel, The role of the secondary fluorophore in ternary plastic scintillators aiming at discriminating fast neutrons from gamma-rays. J. Lumin. **213**, 67–74 (2019)
4. S.W. Moser, W.F. Harder, C.R. Hurlbut, M.R. Kusner, Principles and practice of plastic scintillator design. Radiat. Phys. Chem **41**(1–2), 31–36 (1993)

5. V.A. Li, T.M. Classen, S.A. Dazeley, M.J. Duvall, I. Jovanovic, A.N. Mabe, E.T.E. Reedy, F. Sutanto, A prototype for SANDD: a highly-segmented pulse-shape-sensitive plastic scintillator detector incorporating silicon photomultiplier arrays. Nucl. Instrum. Methods Phys. Res. A **942**, 162334 (2019)

6. N.P. Zaitseva, A.M. Glenn, A.N. Mabe, M.L. Carman, C.R. Hurlbut, J.W. Inman, S.A. Payne, Recent developments in plastic scintillators with pulse shape discrimination. Nucl. Instrum. Methods Phys. Res. A **889**, 97–104 (2018)

7. M.D. Palma, A. Quaranta, T. Marchi, G. Collazuol, S. Carturan, M. Cinausero, M. Degerlier, F. Gramegna, Red emitting phenyl-polysiloxane based scintillators for neutron detection. IEEE Trans. Nucl. Sci. **61**(4), 2052–2058 (2014)

8. M. Hamel, V. Simic, S. Normand, Fluorescent 1, 8-naphthalimides-containing polymers as plastic scintillators. An attempt for neutron–gamma discrimination. React. Funct. Polym. **68**(12), 1671–1681 (2008)

9. B.L. Funt, A. Hetherington, The influence of chain length on the luminescent output of plastic scintillators. Int. J. Appl. Radiat. Isot. **4**, 3–4 (1959)

10. E. Chauveau, Dissertation, Université de Bordeaux **1**, (2010)

11. J. Zhu, C. Deng, H. Jiang, Z. Zheng, R. Gong, Y. Bi, L. Zhang, R. Lin, The impact of fluorescent dyes on the performances of polystyrene-based plastic scintillators. Nucl. Instrum. Methods Phys. Res. A **835**, 136–141 (2016)

12. A.F. Molisch, B.P. Oehry, *Radiation Trapping in Atomic Vapours* (Oxford University Press, Oxford, 1998)

13. A.F. Adadurov, P.N. Zhmurin, V.N. Lebedev, V.D. Titskaya, Optimizing concentration of shifter additive for plastic scintillators of different size. Nucl. Instrum. Methods Phys. Res. A **599**, 2–3 (2009)

14. Y.N. Kharzheev, Radiation hardness of scintillation detectors based on organic plastic scintillators and optical fibers. Phys. Part. Nucl. **50**(1), 42–76 (2019)

15. M.A. Ahmed, R.M. Khafagy, S.T. Bishay, N.M. Saleh, Effective dye removal and water purification using the electric and magnetic $Zn_{0.5}Co_{0.5}Al_{0.5}Fe_{1.46}La_{0.04}O_4$/polymer core–shell nanocomposites. J. Alloys Compd. **578**, 121–131 (2013)

16. M.T. Razzak, S.P. Dewi, H. Lely, E. Taty, The characterization of dressing component materials and radiation formation of PVA–PVP hydrogel. Radiat. Phys. Chem. **55**(2), 153–165 (1999)

17. S.R. Yousefi, D. Ghanbari, N.M. Salavati, Hydrothermal synthesis of nickel hydroxide nanostructures and flame retardant poly vinyl alcohol and cellulose acetate nanocomposites. J. Nanostruct. **6**(1), 77–82 (2016)

18. S.R. Yousefi, A. Sobhani, M. Salavati-Niasari, A new nanocomposite superionic system (CdHgI4/HgI2): synthesis, characterization and experimental investigation. Adv. Powder Technol. **28**(4), 1258–1262 (2017)

19. S.S. Devangamath, B. Lobo, Structural, optical and electrical studies on hybrid material of in situ formed silver sulfide in polymer blend matrix. J. Inorg. Organomet. Polym. Mater. **29**(5), 1466–1475 (2019)

20. A.J. Pai, B.K. Sarojini, K.R. Harshitha, B.S. Holla, A.G. Lobo, Spectral, morphological and optical studies on bischalcone doped polylactic acid (PLA) thin films as luminescent and UV radiation blocking materials. Opt. Mater. **90**, 145–151 (2019)

21. S. Lee, J. Son, D.G. Kim, J. Choi, Y.K. Kim, Characterization of plastic scintillator fabricated by UV LED curing machine. Nucl. Instrum. Methods Phys. Res. A **929**, 23–28 (2019)

22. G.F. Knoll, *Radiation Detection and Measurement* (Wiley, New York, 2010)

23. T. Kamalesh, P. Karuppasamy, M.S. Pandian, P. Ramasamy, S. Verma, Growth of large size triphenylphosphine oxide 4-Nitrophenol (TP4N) single crystal by Sankaranarayanan–Ramasamy (SR) method for third order nonlinear optical applications. Chin. J. Phys. **76**, 68–78 (2022)

24. T. Hasegawa, Advanced multiple-angle incidence resolution spectrometry for thin-layer analysis on a lowrefractive-index substrate. Anal. Chem. **79**(12), 4385–4389 (2007)

25. L.J. Basile, Characteristics of plastic scintillators. J. Chem. Phys. **27**(3), 801–806 (1957)

26. A. Wieczorek, A. Kochanowski. Development of novel plastic scintillators based on polyvinyltoluene for the hybrid J-PET/MR tomograph. arXiv preprint https://arxiv.org/abs/1710.08136 (2017)

27. Organic Scintillation Materials, Saint-Gobain Crystals, Paris, France

28. R.N. Nurmukhametov, L. Volkova, V.G. Klimenko, S.P. Kabanov, R. Salov, Fluorescence and absorption of a polystyrene-based scintillator exposed to UV laser radiation. J. Appl. Spectrosc. **74.6**, 824–830 (2007)

29. Y. Nagumo, K. Okada, T. Tadokoro, Y. Ueno, J. Nukaga, T. Ishitsu, I. Takahashi, Y. Fujishima, K. Hayashi, K. Nagashima, Development of a gamma camera to image radiation fields. Prog. Nucl. Sci. Technol. **4**(1), 14–17 (2014)

30. I. Hossain, N. Sharip, K.K. Viswanathan, Efficiency and resolution of HPGe and NaI (tl) detectors using gamma-ray spectroscopy. Sci. Res. Essays **7**(1), 86–89 (2012)

31. R. Rahmanifard, F. Katebi, A.R. Zahedi, R. Gholipour-Peyvandi, Synthesis and development of a vinyltoluene-based plastic scintillator. J. Lumin. **194**, 456–460 (2018)

32. C.H. Lee, J. Son, T.H. Kim, Y.K. Kim, Characteristics of plastic scintillators fabricated by a polymerization reaction. Nuclear Eng. Technol. **49**(3), 592–597 (2017)

33. B. Richard, Firestone. Table of Isotopes, CD ROM Edition, Version 1.0. (1996)

34. E.V. van Loef, G. Markosyan, U. Shirwadkar, K.S. Shah, Plastic scintillators with neutron/gamma pulse shape discrimination. IEEE Trans. Nucl. Sci. **61**(1), 467–471 (2013)

35. Radiation Detection Scintillators | Crystals (saint-gobain.com)

36. W. Mengesha, P.L. Feng, J.G. Cordaro, M. Anstey, N. Myllenbeck, D.J. Throckmorton. Plastic Scintillators Light Yield Energy Calibration. No. SAND2015-10999J. Sandia National Lab. (SNL-CA), Livermore, CA (United States), (2015)

37. N.Z. Galunov, O.A. Tarasenko, V.A. Tarasov, Determination of the light yield of organic scintillators. Funct. Mater. **20**(3), 304–309 (2013)

38. L. Torrisi, Radiation damage in polyvinyltoluene (PVT). Radiat. Phys. Chem **63**(1), 89–92 (2002)

39. K. Wick, D. Paul, P. Schröder, V. Stieber, B. Bicken, Recovery and dose rate dependence of radiation damage in scintillators, wavelength shifters and light guides. Nucl. Instrum. Methods Phys. Res. B **61**(4), 472–486 (1991)

40. C. Zorn, A pedestrian's guide to radiation damage in plastic scintillators. Nucl. Phys. B **32**, 377–383 (1993)

41. R.-Y. Zhu, Radiation damage in scintillating crystals. Nucl. Instrum. Methods Phys. Res. A **413.2–3**, 297–311 (1998)

42. C. Zorn, M. Bowen, S. Majewski, J. Walker, R. Wojcik, C. Hurlbut, W. Moser, Pilot study of new radiation-resistant plastic scintillators doped with 3-hydroxyflavone. Nucl. Instrum. Methods Phys. Res. A **273**(1), 108–116 (1988)